Review of theoretical gain-optimization studies in 10·6 μm CO_2-N_2 gasdynamic lasers

K P J REDDY and N M REDDY

Department of Aerospace Engineering, Indian Institute of Science, Bangalore 560012, India

Abstract. A comprehensive theoretical analysis of optimization of gain in CO_2-N_2 gasdynamic laser employing wedge or conical or hyperbolic nozzles with either H_2O or He as the catalyst is presented. After a review of previous work, the usual governing equations for the steady inviscid quasi-one-dimensional flow in a supersonic nozzle of a gasdynamic laser are used to obtain similar solutions for the various flow quantities, which variables are subsequently used to optimize the small-signal gain on the $P(20)$ line of the $(001) \rightarrow (100)$ transition of CO_2 at wavelength 10·6 μm. The corresponding optimum values like reservoir pressure and temperature and nozzle area ratio also have been predicted and presented in the form of graphs. The analysis predicts that employing of 2D-wedge nozzle results in higher gain values and the CO_2-N_2-H_2O gasdynamic laser employing 2D-wedge nozzle is operationally the best laser system for which the optimum value as high as 3·1 m^{-1} gain can be obtained.

Keywords. CO_2-N_2 gasdynamic laser; gain-optimization; similar solutions; universal equations; supersonic nozzles.

PACS No. 42·55

1. Introduction

In the mid 1960s the conventional electric discharge CO_2 laser was the only high power gas laser operating on a practical basis. Simple scale-up of N_2-CO_2 electric discharge lasers led to output powers in multikilowatt range with lasers which were hundreds of feet in length—about 9 kW output power was obtained from laser tubes of about 200 ft long. Thus, although high powers could be obtained, the lasers became very cumbersome because of the necessity of large dimensions of the laser tube. In addition the discharge pumping of CO_2 is limited by simultaneous heating of the gas which thermally populates the lower laser level, thus reducing or even destroying the population inversion, hence terminating the laser action. Although this objection can be partly overcome by flowing the gas at high speeds, the wastage energy resulting from inefficient operation eventually sets a limit on the average power output that can be obtained from the discharge pumped lasers. These difficulties were eventually circumvented by the invention of gasdynamic lasers (GDL) which have created a breakthrough in high power laser technology.

The idea of creating population inversion in molecular systems by rapid heating or cooling of the system was first suggested by Basov and Oraevskii (1963). Achieving of cooling and population inversions by rapid non-equilibrium expansion of an initially hot gas through a supersonic nozzle was subsequently suggested by Hurle and

Hertzberg (1965) who considered a specific case of electronic level inversions in expanding Xe but were unsuccessful in measuring such inversions in the laboratory. The possibility of population inversion in CO_2-N_2 mixtures by similar rapid expansion through a supersonic nozzle was suggested by Konyukhov and Prokhorov (1966). Combining these ideas with his previous idea of production of vibrational non-equilibrium in CO_2 in a high-speed flow, Kantrowitz (1946) operated the first GDL in 1966, alongwith the group of engineers and scientists at the Avco Everett Research Laboratory, using a mixture of CO_2-N_2-H_2O (Gerry 1970). To date the GDL using CO, N_2O, CS_2, HCl and DCl as active media have been created. However, CO_2-N_2 GDL using H_2O or He as the catalyst is the most widely studied laser, since it operates efficiently in the IR region of high interest and also produces output powers of tens and hundreds of kilowatts.

Since this early progress, the work on GDL has attracted international interest both experimentally and theoretically. It is now well over a decade, since the first reports about CO_2 GDL performance appeared, laboratory experiments have been performed using arc tunnels, shock tunnels and combustion driven devices. Numerous theoretical calculations ranging from sophisticated computer programs to quick approximate analyses of the performance of GDL have been reported. A detail survey of these efforts is presented in the form of review papers by Anderson (1975) and Christiansen et al (1975) and also in the form of books by Anderson (1976) and Losev (1981). In general, the GDL performance is characterized through the small-signal optical gain and optical power output parameters. It is evident from many investiga-tions reported that the performance characteristics of a GDL depend on a large number of parameters like mixture composition, initial conditions (pressure P_0 and tempera-ture T_0 at the reservoir), size and contour of the nozzle, etc. To choose optimal operating conditions for a GDL we must know how these parameters affect its characteristics. This problem is usually studied by varying (in theory or experiment) a certain parameter independently, keeping the other parameters constant. However, making an exhaustive study of the influence of these parameters on the GDL performance would indeed be very formidable because of the large number of parameters involved. The only best way is to optimize many parameters simultaneously.

No work has been reported so far on the problem of simultaneous optimiziation except for the publication by Losev and Makarov (1975). They carried out the analysis for two dimensional wedge nozzle by varying the reservoir conditions, mixture composition and nozzle geometry and by applying an optimum seeking method. However, they have obtained the results for only a specific nozzle configuration and a selected set of mixture composition. More recently, Mcmanus and Anderson (1976) presented a closed-form engineering correlation for the peak small-signal gain encompassing a wide range of GDL parameters, which could be used for a quick estimation of the peak value of small-signal gain for any given set of parameters. But it is not possible to predict what combination of these GDL parameters would yield the optimum value for the small-signal gain from this correlation.

Hence, there is a need for the systematic analysis of the optimization of the GDL performance by simultaneous optimization of many GDL parameters. The main contribution of the present work centres on the fact that we have been able to perform such an analysis for a wide range of mixture compositions and for different nozzle contours like, wedge, conical and hyperbolic (Reddy and Shanmugasundaram 1979a). The equations governing the steady, inviscid quasi-one-dimensional flow in the given

nozzle of the GDL are reduced to a universal form so that their solutions depend on a single unifying parameter (which combines all the other parameters of the problem). These equations are solved numerically to obtain similar solutions for various flow quantities, which variables are subsequently used to optimize the small-signal gain. The corresponding optimum values like reservoir pressure and temperature and nozzle area ratio are also computed using these solutions. Our results presented in the form of graphs have made it possible to draw up a comprehensive prescription for optimizing the GDL performance and these should be of considerable assistance in the optimization of CO_2-N_2 GDL using H_2O or He as catalyst.

Since our work on optimization studies has been presented in the form of a series of published papers (Reddy and Shanmugasundaram 1979a, b, c; Shanmugasundaram and Reddy 1980, 1983; Reddy and Reddy 1984) and unpublished departmental reports (Reddy and Shanmugasundaram 1977, Shanmugasundaram and Reddy 1977, 1979; Reddy and Reddy 1982), which are not easily accessible to a reader, it is the aim of this paper to present a comprehensive review of our work on theoretical optimization studies of gain in CO_2-N_2 GDL. All the important results obtained for both the GDL systems, CO_2-N_2-H_2O and CO_2-N_2-He, for different nozzle configurations, wedge and conical or hyperbolic, are presented here. The results are computed for a wide range of gas mixture compositions in both the systems and are presented in the form of graphs. But, since the number of graphs is very large, we have presented here only a few important graphs for representative gas compositions. If one wants to get optimum operating parameters for a whole range of gas compositions in a particular GDL system, they could be obtained by referring to a corresponding earlier publications. One of the main features of the present review is that it leads to the prediction of the best operating GDL system for a given nozzle contour.

In §2, the fundamental governing equations for the steady inviscid quasi-one-dimensional flow in a supersonic nozzle of a GDL are introduced in their universal form. This section also contains the expressions for the population inversion and the small-signal optical gain of the laser system. The numerical solutions of the governing equations are presented in §3 along with the results and overall conclusions are summarized in §4.

2. Governing equations

The governing equations for the steady inviscid quasi-one-dimensional flow in a supersonic nozzle of a GDL are the usual global mass, momentum and energy conservation equations and the equation of state. In addition, for a non-reacting mixture of gases like that in a GDL where only the vibrational non-equilibrium is of importance, the equations governing vibrational energy exchange through bimolecular collisions are to be considered. For CO_2-N_2-H_2O or He GDL the number of such vibrational energy exchange reactions is very large with not all the reaction rates known very well, which makes the problem all the more difficult. However, the problem is simplified by the approximate two-temperature model for the vibrational kinetics of CO_2-N_2 system, introduced by Anderson (1970) based on certain observations on the molecular-energy exchange reactions involved. Figure 1 shows the two-temperature vibrational model, including various vibrational levels and their energies. In the present analysis we adopt the two temperature model as shown in figure 1, where mode I (of
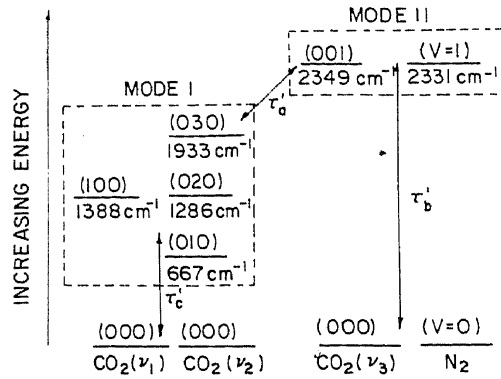
Figure 1. Schematic of Anderson's vibrational model.

vibrational temperature T_I) and mode II (of vibrational temperature T_{II}) include respectively the lower and upper laser levels of the system and τ_a', τ_b', and τ_c' are the effective relaxation times of these modes.

Two more algebraic equations, for the population inversion and the small-signal optical gain which could be obtained from the foregoing equations are to be considered for GDL studies. Thus, the number of equations to be considered becomes eight, consisting of the three conservation equations, the equation of state, the two rate equations governing the vibrational relaxation of the two modes, and the two algebraic equations for population inversion and optical gain.

2.1 Generalized momentum and vibrational rate equations

To start with, the governing equations are in their dimensional form which are given in full detail in (Reddy and Shanmugasundaram 1979a). These equations are first normalized with respect to a chosen set of reference values and then transformed into a similar form by using a new independent variable η, which is a function of the normalized density. For a given gas mixture and a family of nozzle shapes, the solutions of these equations depend on two parameters S_0 and λ_I, where the latter is defined in terms of all the other parameters of the problem. These similar equations are then reduced to a universal form, by transforming the independent variable η to a new variable ξ, so that the solutions depend on a single parameter χ_I. Then the universal equations governing the normalized translational temperature and vibrational temperatures of two modes I and II in terms of the independent variable ξ are of the form (Reddy and Shanmugasundaram 1979a),

$$\psi - \alpha \frac{d\psi}{d\xi} - X_C \sum_{m=I,II} \overline{G}_m \frac{d\phi_m}{d\xi} = 0, \tag{1}$$

$$\frac{d\phi_m}{d\xi} = \frac{K_m \psi}{N_s} \exp\left[\chi_m + \xi(1 - 1/ij)\right.$$

$$\left. - B_{qq} \psi^{-1/3}\right]\left[\frac{\overline{E}_e - \overline{E}}{G}\right]_m, \tag{2}$$

where, the subscript e refers to local equilibrium and $q = C$ for $m = I$ and $q = N$ for $m = II$, where C and N denote, respectively, CO_2 and N_2. Equation (1) represents the

generalized momentum equation obtained by combining the momentum and energy conservation equations and the equation of state. Equation (2) represents the rate equation (of the Landau-Teller type) governing the relaxation of the vibrational energy of mode m. The normalized translational temperature, $\psi = T'/\theta'_{v_N}$, and the vibrational temperatures for modes I and II, $\phi_m = T'_m/\theta'_{v_N}$, are normalized with respect to θ'_{v_N} ($= 3357°K$), the characteristic temperature for the normal vibrational mode for N_2, where the primes denote dimensional quantities. The quantity $\alpha = [2·5(X_C + X_N) + 0·5nX_H]$ where n is the number of degrees of freedom of the catalyst and X_C, X_N and X_H are, respectively, the mole fractions of CO_2, N_2 and the catalyst H_2O or He. The parameters i and j govern the shape of the nozzle whose normalized cross-sectional area ratio is given by

$$A = (1 + x^j)^i;$$

for example, $i = 1, j = 1$ for wedge nozzles, $i = 2, j = 1$ for conical nozzles and $i = 1$, $j = 2$ for hyperbolic nozzles.

The various functions occurring in (1) and (2) are:

$$\bar{E}_I = \frac{\bar{\theta}_{v_1}}{\exp(\bar{\theta}_{v_1}/\phi_I) - 1} + \frac{2\bar{\theta}_{v_2}}{\exp(\bar{\theta}_{v_2}/\phi_I) - 1}, \tag{3}$$

$$\bar{E}_{II} = \frac{\bar{\theta}_{v_3}}{\exp(\bar{\theta}_{v_3}/\phi_{II}) - 1} + \frac{X_N/X_C}{\exp(1/\phi_{II}) - 1}, \tag{4}$$

$$\bar{G}_I = (\bar{\theta}_{v_1}/\phi_I)\frac{\exp(\bar{\theta}_{v_1}/\phi_I)}{[\exp(\bar{\theta}_{v_1}/\phi_I) - 1]^2} + 2(\bar{\theta}_{v_2}/\phi_I)^2\frac{\exp(\bar{\theta}_{v_2}/\phi_I)}{[\exp(\bar{\theta}_{v_2}/\phi_I) - 1]^2}, \tag{5}$$

$$\bar{G}_{II} = (\bar{\theta}_{v_3}/\phi_{II})^2\frac{\exp(\bar{\theta}_{v_3}/\phi_{II})}{[\exp(\bar{\theta}_{v_3}/\phi_{II}) - 1]^2}$$

$$+ (X_N/X_C)(1/\phi^2_{II})\cdot\frac{\exp(1/\phi_{II})}{[\exp(1/\phi_{II}) - 1]^2}, \tag{6}$$

$$K_I = X_C + X_N[(\tau'_c)_{CC}/(\tau'_c)_{CN}] + X_H[(\tau'_c)_{CC}/(\tau'_c)_{CH}], \tag{7}$$

$$K_{II} = [X_C K_a(\tau'_b)_{NN}/(\tau'_a)_{CC} + X_N K_b]/(X_C + X_N) \tag{8}$$

where

$$K_a = X_C + X_N[(\tau'_a)_{CC}/(\tau'_a)_{CN}] + X_H[(\tau'_a)_{CC}/(\tau'_a)_{CH}], \tag{9}$$

$$K_b = X_C[(\tau'_b)_{NN}/(\tau'_b)_{NC}] + X_N + X_H[(\tau'_b)_{NN}/(\tau'_b)_{NH}] \tag{10}$$

In the above equations, $\bar{\theta}_{v_p} = \theta'_{v_p}/\theta'_{v_N}$, $p = 1, 2, 3$ ($\theta'_{v_1} = 1999°K$; $\theta'_{v_2} = 960°K$; $\theta'_{v_3} = 3393°K$) are the normalized characteristic temperatures for the three vibrational modes of CO_2. The τ's in (7)–(10) are the vibrational relaxation times for various collisional partners. The simplified correlations for the relaxation times τ'_a, τ'_b, and τ'_c for various collisional partners are listed in Appendix A of reference (Reddy and Shanmugasundaram 1979a).

The independent parameter ζ and the universal parameter χ_m given in (1) and (2) are defined as

$$\zeta = S_0 + \ln\rho \tag{11}$$

and

$$\chi_m = \ln\left[\frac{p'_0 L'\theta'_{v_N}(\rho_* u_*)^{a + 1/ij}}{ij(R'_M)^{1/2}(T'_0)^{3/2}J_{qq}}\right] - (1 - 1/ij)S_0, \tag{12}$$

where $\rho = \rho'/\rho'_0$ is the normalized density, u is the normalized velocity, p'_0 and T'_0 are the reservoir pressure and temperature, R'_M is the mixture gas constant, $L' = r'_*/\tan \delta$ is the nozzle shape parameter where $2r'_*$ is the throat diameter and 2δ is the expansion angle. The exponent a is equal to 6 for conical or hyperbolic and 7·2 for wedge nozzle. The subscripts '0' and '*' refers to the reservoir conditions and the conditions at the nozzle throat. The constants B's and J's occurring in (2) and (12) are constants calculated from the vibrational relaxation times and are independent of the catalyst used. Their values are

$$B_{CC} = 2\cdot7389; \quad J_{CC} = 1\cdot555 \times 10^{-8} \text{ atm-sec};$$
$$B_{NN} = 14\cdot3098; \quad J_{NN} = 2\cdot450 \times 10^{-11} \text{ atm-sec}.$$

The quantity S_0 is the specific entropy and is given by

$$S_0 = -\ln \rho_e + \alpha \ln \psi_e + \frac{X_C}{\psi_e} [\overline{E}_I + \overline{E}_{II}]_e$$
$$- X_C \ln \{ [1 - \exp(-\overline{\theta}_{v_1}/\psi)]$$
$$\times [1 - \exp(-\overline{\theta}_{v_2}/\psi)]^2 [1 - \exp(-\overline{\theta}_{v_3}/\psi)]$$
$$\times [1 - \exp(-1/\psi)]^{(X_N/X_C)} \}_e + S_r \tag{13}$$

where S_r is the reference entropy and is equal to 26·3 for He and 29·57 for H_2O catalyst when wedge nozzle is used and 26·47 for He and 29·64 for H_2O catalyst when conical or hyperbolic nozzle is used. Equation (13) is nothing but the condition of vibrational equilibrium (represented by suffix e) and is obtained as a limiting case of the non-equilibrium processes governed by (1) and (2). It is also an expression for the conservation of entropy in an adiabatic flow.

The mass flow factor $\rho_* u_*$ and the normalized density ρ_* occurring in (12) have been correlated as functions of reservoir temperature and are given by (Reddy and Shanmugasundaram 1979a)

$$\rho_* u_* = 0\cdot689 - 6\cdot3 \times 10^{-6} T'_0 (^\circ K) = k_1$$
$$\rho_* = 0\cdot634 - 2\cdot33 \times 10^{-6} T'_0 (^\circ K) = k_2 \tag{14}$$

for the conical or hyperbolic nozzle, and

$$\rho_* u_* = 0\cdot686 - 8\cdot0 \times 10^{-6} T'_0 (^\circ K) = k_1 \text{ (for He catalyst)}$$
$$= 0\cdot66 = k_1 \text{ (for } H_2O \text{ catalyst)}$$
$$\rho_* = 0\cdot63 = k_2 \tag{15}$$

for the wedge nozzle.

The normalized velocity ratio (u/u_*) along the nozzle axis has also been correlated as a function of the normalized area ratio $A = A'/A'_*$ and is given by (Reddy and Shanmugasundaram 1979a)

$$(u/u_*) = k_1^{-4} [0\cdot5 - 0\cdot31(1 + \log_{10} A)^{-2}] \tag{16}$$

for conical or hyperbolic nozzle and

$$(u/u_*) = k_1^{-3\cdot37} [-0\cdot022 + 0\cdot049(0\cdot3 + \log_{10} A)^{-1\cdot5}] \text{ for } M < 1$$
$$= k_1^{-3\cdot37} [1\cdot165 - 0\cdot56(0\cdot1 + \log_{10} A)^{-0\cdot2}] \text{ for } M \geq 1$$

or

$$(u/u_*) = k_1^{-3\cdot98}[-0\cdot0217 + 0\cdot0399(0\cdot234 + \log_{10} A)^{-1\cdot197}] \text{ for } M < 1$$
$$= k_1^{-3\cdot98}[0\cdot669 - 0\cdot216(0\cdot194 + \log_{10} A)^{-0\cdot467}] \text{ for } M \geqslant 1 \quad (17)$$

for He or H_2O catalyst respectively for the family of wedge nozzles. All these correlations are obtained by using the computer program of Lordi *et al* (1966) and further details may be found in the paper by Reddy and Shanmugasundaram (1979a).

2.2 *Population inversion and small-signal optical gain*

We consider the $P(20)$ transition at a wavelength of $10\cdot6$ μm and occurring between $J = 19$ rotational level of (001) and $J = 20$ rotational level of (100) vibrational levels of CO_2. Assuming that the optical line is homogeneously broadened, we have the following algebraic equations for population inversion (PI) and the small-signal optical gain (G_0) as functions of the flow quantities.

$$PI = \frac{\exp(-\bar{\theta}_{v_3}/\phi_{II}) - \exp(-\bar{\theta}_{v_1}/\phi_I)}{\bar{Q}_{vib}} \quad (18)$$

and

$$G_0/m = 9\cdot77 \frac{(PI)}{P(x_i)\psi^{3/2}} \exp\left(\frac{0\cdot0703}{\psi}\right) \quad (19)$$

where

$$\bar{Q}_{vib} = [1 - \exp(-\bar{\theta}_{v_1}/\phi_I)]^{-1}[1 - \exp(-\bar{\theta}_{v_2}/\phi_I)]^{-2}$$
$$\times [1 - \exp(-\bar{\theta}_{v_3}/\phi_{II})]^{-1} \quad (20)$$

and

$$P(x_i) = 1 + 0\cdot7589(X_N/X_C) + b(X_H/X_C) \quad (21)$$

with $b = 0\cdot3836$ for H_2O and $b = 0\cdot6972$ for He catalyst.

2.3 *Non-similar function N_s*

The quantity N_s occurring in (2) is called the non-similar function defined as

$$N_s = \mp(M^2/M^2 - 1)(1 - A^{-1/i})^{(j-1)/j} u^{(1+1/ij)} (\rho_* u_*)^6$$

where M is the Mach number and u is the local velocity. The function N_s is computed for the actual laser gas mixtures of CO_2-N₂-H₂O or He in GDL systems using conical or hyperbolic or wedge nozzles by using the computer program given by Lordi *et al* (1966, unpublished). We have found that the variation of N_s is very small for different reservoir pressures but its variation with reservoir temperature is noticeable. Thus, the function N_s is computed for the reservoir temperatures of 1000, 1500, 2000, 2500 and 3000°K at a reservoir pressure of 10 atm, for a wide range of gas compositions. It is found that for a particular reservoir temperature, the N_s variation is negligible for different gas compositions in a given nozzle. These values of N_s are plotted as functions (ξ_*/ξ) where ξ_* is the value of ξ at the nozzle throat, for each composition at different temperatures. A mean curve is computed from these large number of curves which represents the final correlation for the non-similar function N_s. These final correlations for the gas mixtures of CO_2-N₂-H₂O and CO_2-N₂-He and for three different nozzle shapes are presented in figure 2. The mean correlations can be also represented by simple analytical equations
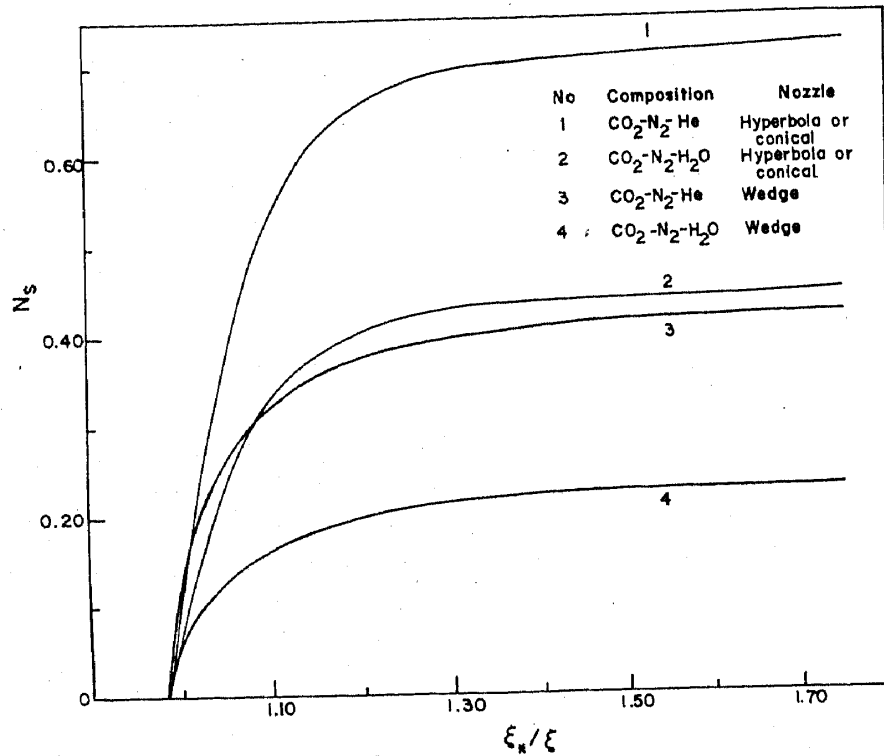
Figure 2. Correlations of function N_s.

of the form:

$$N_s = 0 \text{ for } (\xi_*/\xi) \leqslant 0.988,$$
$$= 0.030 - 12.5(0.995 - \xi_*/\xi)^{1.208}, \text{ for } 0.988 < (\xi_*/\xi) \leqslant 0.995$$
$$= 0.45 - 5.7 \times 10^3 (\xi_*/\xi - 0.5)^{-6.134}, \text{ for } (\xi_*/\xi) > 0.995 \quad (22)$$

for H_2O catalyst and

$$N_s = 0 \text{ for } (\xi_*/\xi) \leqslant 0.983$$
$$= 0.045 - 3(0.993 - \xi_*/\xi)^{0.906}, \text{ for } 0.983 < (\xi_*/\xi) \leqslant 0.993$$
$$= 0.722 - 0.84 \times 10^{25} (\xi_*/\xi + 2.8)^{-43.334}, \text{ for } (\xi_*/\xi) > 0.993 \quad (23)$$

for He catalyst.
The correlations given by (22) and (23) are for the conical or hyperbolic nozzles.
Similarly, for the wedge nozzles we have

$$N_s = 0 \text{ for } (\xi_*/\xi) \leqslant 0.985$$
$$= 0.039 - 0.118(0.995 - \xi_*/\xi)^{0.241}, \text{ for } 0.985 < (\xi_*/\xi) \leqslant 0.995$$
$$= 0.233 - 4.41 \times 10^{-3} (\xi_*/\xi - 0.816)^{-2.186}, \text{ for } (\xi_*/\xi) > 0.995 \quad (24)$$

for H_2O catalyst and

$$N_s = 0 \text{ for } (\xi_*/\xi) \leqslant 0.985$$
$$= 0.088 - 0.682(0.995 - \xi_*/\xi)^{0.45}, \text{ for } 0.985 < (\xi_*/\xi) \leqslant 0.995$$
$$= 0.436 - 8.6 \times 10^{-3} (\xi_*/\xi - 0.85)^{-1.9} \text{ for } (\xi_*/\xi) > 0.995 \quad (25)$$

for He catalyst.

Equations (1) and (2) are the basic equations governing the vibrational non-equilibrium gas flow in the GDL and since PI and G_0 as given by (18) and (19), are only functions of the gas composition and ϕ_I, ϕ_{II} and ψ, the main emphasis here would be on obtaining the solutions for the last three variables. Since, the solutions of (1) and (2) for a given composition and a value of ij depend on only one parameter χ_I, which combines all the other parameters of the system, the solutions thus obtained will be universal for a given gas mixture and family of nozzle shapes (given ij).

3. Results and discussion

For a given laser mixture composition, (1) and (2) are solved simultaneously for the three unknowns ϕ_I, ϕ_{II} and ψ, with χ_I as the parameter (since $\chi_{II} = \chi_I + \ln(J_{CC}/J_{NN})$) and for any value of ij. In the present paper we consider both the values $ij = 1$, which represents a wedge nozzle and $ij = 2$, which represents a conical or hyperbolic nozzle. The numerical integration is carried out using the modified, fourth-order RKG method. Since the flow in a GDL starts from a reservoir wherein the hot gas mixture is in equilibrium, the initial values for the three temperatures correspond to this equilibrium state; then, (11) readily gives the appropriate value of ξ at the reservoir. The procedure followed for obtaining numerical solutions is given in detail by Shanmugasundaram and Reddy (1983). The ξ_* value is estimated from (11) by using the ρ_* values as given by (14) or (15) and with a known value of S_0 from the reservoir conditions. At every point along the nozzle, that is for every value of ξ, we calculate ξ_*/ξ and the corresponding value of N_s from any one of the equations (22) to (25) depending upon the system and the nozzle shape considered. If $N_s = 0$, which means the flow is in local vibrational equilibrium, we iteratively solve (13) for ψ_e as a function of ξ. For any other value of $N_s > 0$, implying the prevalence of non-equilibrium conditions within the nozzle, we solve (1) and (2) for the three unknowns ϕ_I, ϕ_{II} and ψ; the appropriate initial values would correspond to the ψ_e value obtained at the last step of the local equilibrium conditions. Knowing the temperature distributions along the nozzle, PI and G_0 as functions of ξ can be calculated from (18) and (19).

In this section the numerical results are presented for the laser fluid including both CO_2-N_2-H_2O (to be called system 1) and CO_2-N_2-He (to be called system 2) gas mixtures. Computations have been carried out for a wide range of compositions, the details of which are given in tables 1 and 2. Solutions for few sample cases of system 1

Table 1. Values of N$_2$ mole fraction in the CO$_2$-N$_2$-H$_2$O laser mixture.

X_{CO_2}	X_{H_2O}						
	0·01	0·02	0·03	0·04	0·06	0·08	0·10
0·05	0·94	0·93	0·92	0·91	0·89	0·87	0·85
0·10	0·89	0·88	0·87	0·86	0·84	0·82	0·80
0·15	0·84	0·83	0·82	0·81	0·79	0·77	0·75
0·20	0·79	0·78	0·77	0·76	0·74	0·72	0·70
0·25	0·74	0·73	0·72	0·71	0·69	0·67	0·65

Table 2. Values of N_2 mole fraction in the CO_2-N_2-He laser mixture.

X_{He}	X_{CO_2}						
	0·025	0·050	0·075	0·10	0·15	0·20	0·25
0·2	0·775	0·75	0·725	0·7	0·65	0·6	0·55
0·3	0·675	0·65	0·625	0·6	0·55	0·5	0·45
0·4	0·575	0·55	0·525	0·5	0·45	0·4	0·35
0·5	0·475	0·45	0·425	0·4	0·35	0·3	0·25
0·6	0·375	0·35	0·325	0·3	0·25	0·2	0·15
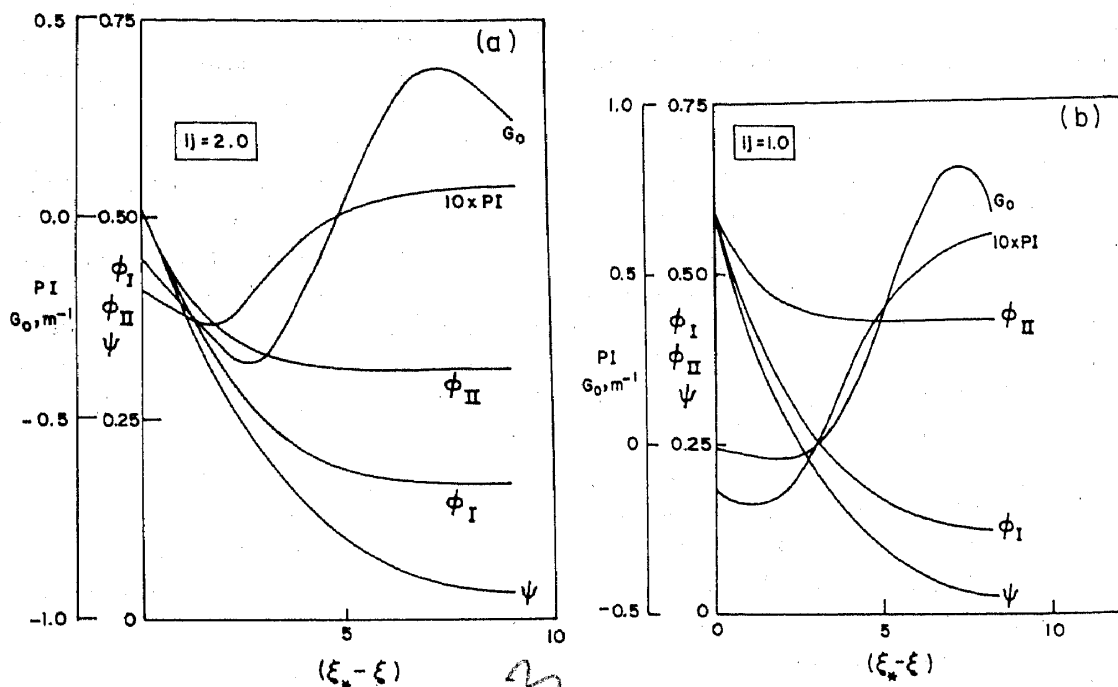
Figure 3. Variation of flow quantities along the GDL nozzle for a. $X_{CO_2} : X_{N_2} : X_{H_2O}$ $= 0\cdot2 : 0\cdot76 : 0\cdot04$; $ij = 2$; $\chi_I = -9$; $\psi_* = 0\cdot575$; $\xi_* = 29\cdot2194$, and b. $X_{CO_2} : X_{N_2} : X_{H_2O}$ $= 0\cdot05 : 0\cdot94 : 0\cdot01$; $ij = 1$; $\chi_I = 4\cdot48$; $\psi_* = 0\cdot601$; $\xi_* = 29\cdot115$.

and 2 for conical or hyperbolic and wedge nozzle shapes are presented in figures 3 and 4. One of the interesting common features of these results is the peaking of G_0 while PI tends to remain constant far downstream of the throat. The reason for the latter trend is the early freezing of the upper laser level (mode II) while the lower level (mode I) freezes sufficiently far downstream of the nozzle throat. The small-signal gain G_0 attains a maximum because of the peaking tendency of the rotational contribution. These effects are discussed in detail by Reddy and Shanmugasundaram (1979b).

For each gas composition, such peak values of G_0 are computed for a range of χ_I values and are plotted in figures 5 and 6. Since the total number of graphs is very large, we have presented the results for only a few compositions in these two figures. Once again, for every gas mixture G_0 attains a maximum value corresponding to a particular
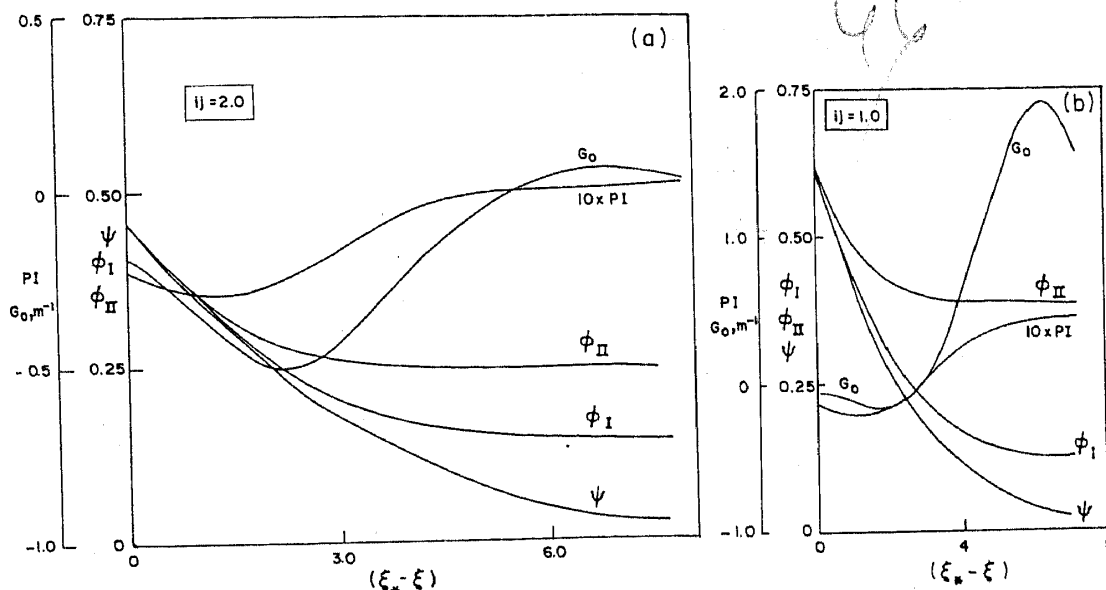
Figure 4. Variation of flow quantities along the GDL nozzle for **a.** $X_{CO_2} : X_{N_2} : X_{He}$ $= 0.25 : 0.55 : 0.2$; $ij = 2$; $\chi_I = -5.5$; $\psi_* = 0.525$; $\xi_* = 25.962$, and **b.** $X_{CO_2} : X_{N_2} : X_{He}$ $= 0.15 : 0.35 : 0.5$; $ij = 1$; $\chi_I = 4.5$; $\psi_* = 0.625$; $\xi_* = 26.36$.
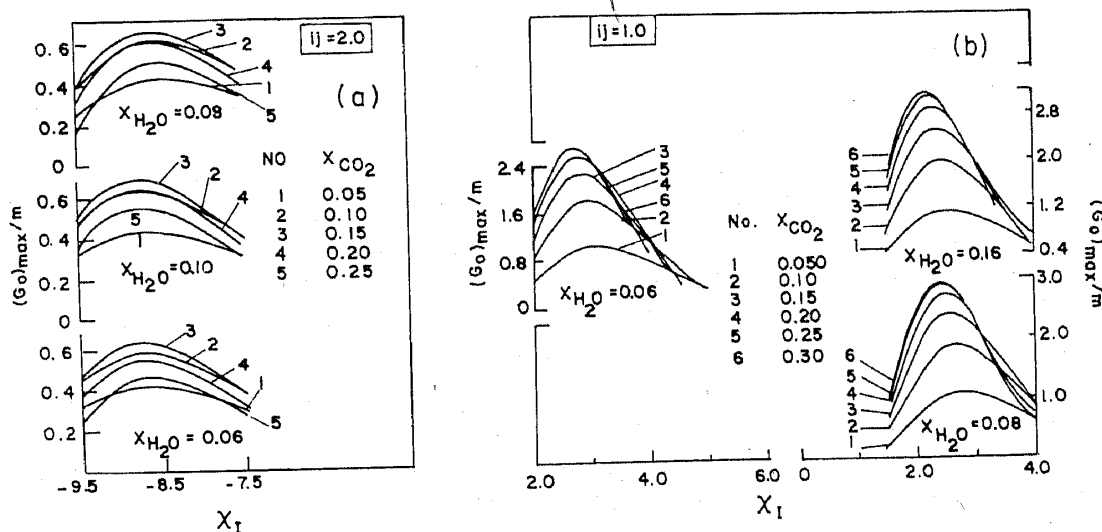

Figure 5. Variation of maximum values of small-signal gain on the $P(20)001 \rightarrow 100$ transition with χ_I for various mixture compositions in system 1 and for **a.** $ij = 2$ and **b.** $ij = 1$.

value of χ_I, and we designate these two quantities as $(G_0)_{opt}$ and $(\chi_I)_{opt}$. Thus for a given laser mixture, $(G_0)_{opt}$ represents the highest possible value of the small-signal optical gain coefficient on the $P(20)$ transition at $10.6 \,\mu m$. There could be larger gain coefficients on other $P(20)$ $(001) \rightarrow (100)$ vibrational-rotational levels. The present analysis could be extended to compute the optimum values on the entire set of P-branch transitions.

It is important to study the dependence of $(G_0)_{opt}$ on CO_2, H_2O and He contents in the laser gas mixture and to achieve this we have cross-plotted these quantities in figures

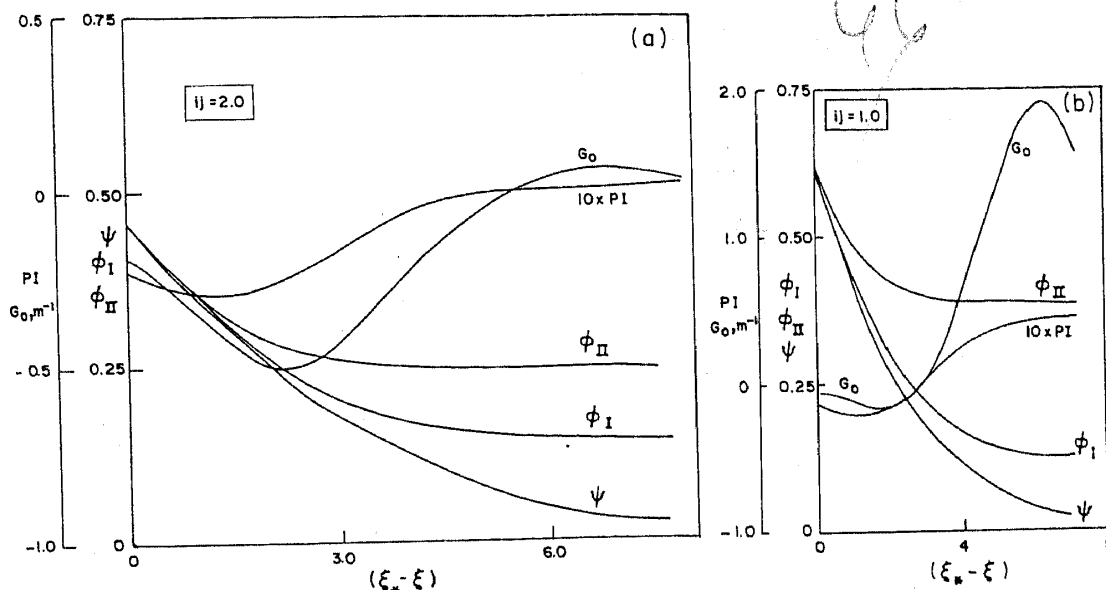**Figure 4.** Variation of flow quantities along the GDL nozzle for **a.** $X_{CO_2}:X_{N_2}:X_{He}$ $= 0.25:0.55:0.2$; $ij = 2$; $\chi_I = -5.5$; $\psi_* = 0.525$; $\xi_* = 25.962$, and **b.** $X_{CO_2}:X_{N_2}:X_{He}$ $= 0.15:0.35:0.5$; $ij = 1$; $\chi_I = 4.5$; $\psi_* = 0.625$; $\xi_* = 26.36$.
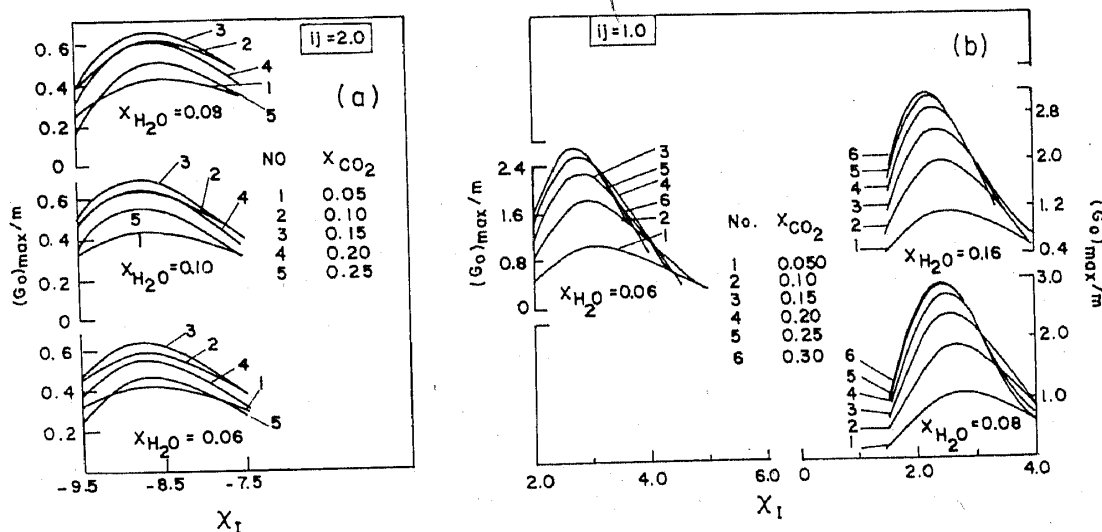

Figure 5. Variation of maximum values of small-signal gain on the $P(20)001 \rightarrow 100$ transition with χ_I for various mixture compositions in system 1 and for **a.** $ij = 2$ and **b.** $ij = 1$.

value of χ_I, and we designate these two quantities as $(G_0)_{opt}$ and $(\chi_I)_{opt}$. Thus for a given laser mixture, $(G_0)_{opt}$ represents the highest possible value of the small-signal optical gain coefficient on the $P(20)$ transition at $10.6\ \mu m$. There could be larger gain coefficients on other $P(20)$ $(001) \rightarrow (100)$ vibrational-rotational levels. The present analysis could be extended to compute the optimum values on the entire set of P-branch transitions.

It is important to study the dependence of $(G_0)_{opt}$ on CO_2, H_2O and He contents in the laser gas mixture and to achieve this we have cross-plotted these quantities in figures
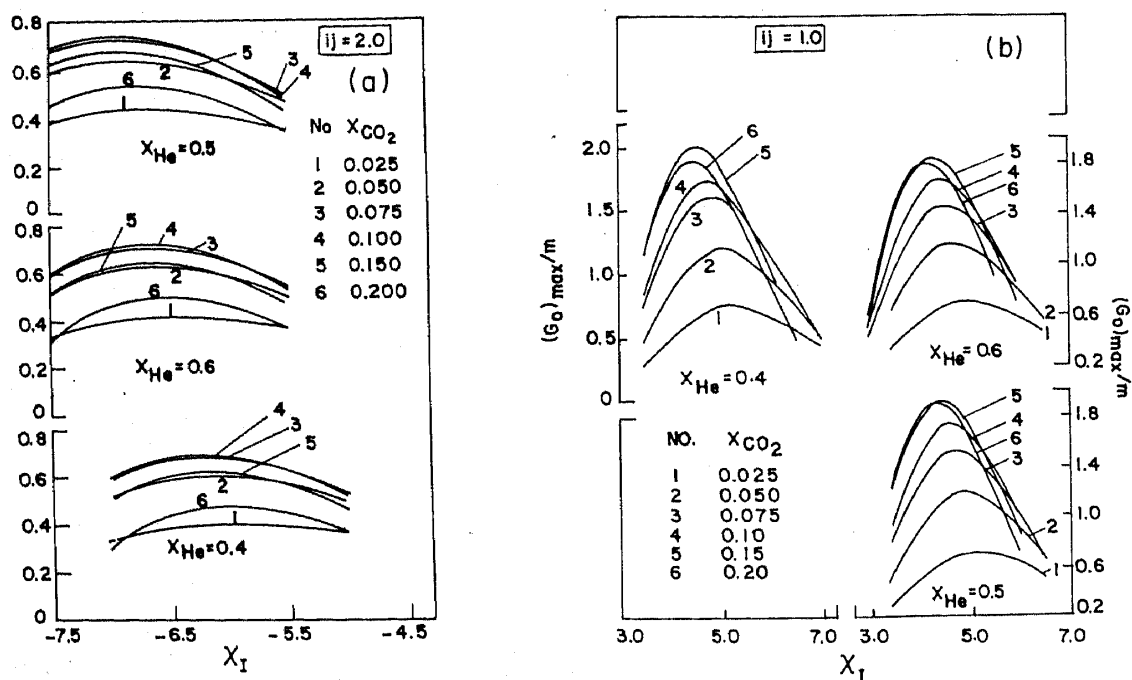
Figure 6. Variation of maximum values of small-signal gain on the $P(20)$ $001 \rightarrow 100$ transition with χ_I for various mixture compositions in system 2 and for **a.** $ij = 2$ and **b.** $ij = 1$.

7 and 8 for both the systems using different nozzle shapes. Here also, we see that $(G_0)_{opt}$ attains a maximum value at some value of CO_2 mole fraction for a given value of H_2O or He content. This value of CO_2 at which $(G_0)_{opt}$ attains a maximum, increases with increasing H_2O or He content. This dependence may be due to a combination of facts like (a) the decrease in the N_2 content because of the increase in the mole fraction of CO_2, with a consequent adverse effect on the "pumping reaction" which is essential for populating the upper laser level and (b) the effectiveness of increasing concentration of the CO_2 molecules itself in the collisional deactivation of the upper laser level.

Figures 7 and 8 also show the tendency of $(G_0)_{opt}$ to peak around 10 mole % of H_2O in system 1 for both wedge and conical or hyperbolic nozzles and at around 40 and 50 mole % of He in system 2 for wedge and conical or hyperbolic nozzles, respectively. The reason for such peaking of $(G_0)_{opt}$ is that as the catalyst number density increases, besides the lower laser level, which is rapidly deexcited by the catalyst, the upper laser level population is also affected adversely, with a result that the PI (and hence G_0) is reduced. From the foregoing results we conclude that very high values for small-signal optical gain could be achieved. Similarly the variation of $(\chi_I)_{opt}$ with respect to CO_2, H_2O and He contents in the laser gas mixture could be studied by cross-plotting $(\chi_I)_{opt}$ vs X_{H_2O}/X_{CO_2} and X_{He}/X_{CO_2}.

After computing the optimum values of G_0 and χ_I as functions of the mole fractions of CO_2 and H_2O or He, the optimum operating parameters like T'_0 and p'_0 for a given laser mixture composition can be easily estimated. Since χ_I, as given by (12), is a function of p'_0, T'_0 and L' by using the $(\chi_I)_{opt}$ value, a range of p'_0 and T'_0 values with L' as a parameter can be obtained for a given gas mixture. However, since L' itself is a function of both the throat height and the expansion angle of the nozzle, to have more flexibility in estimating the reservoir pressure for any desired value of L', $p'_0 L'$ is directly
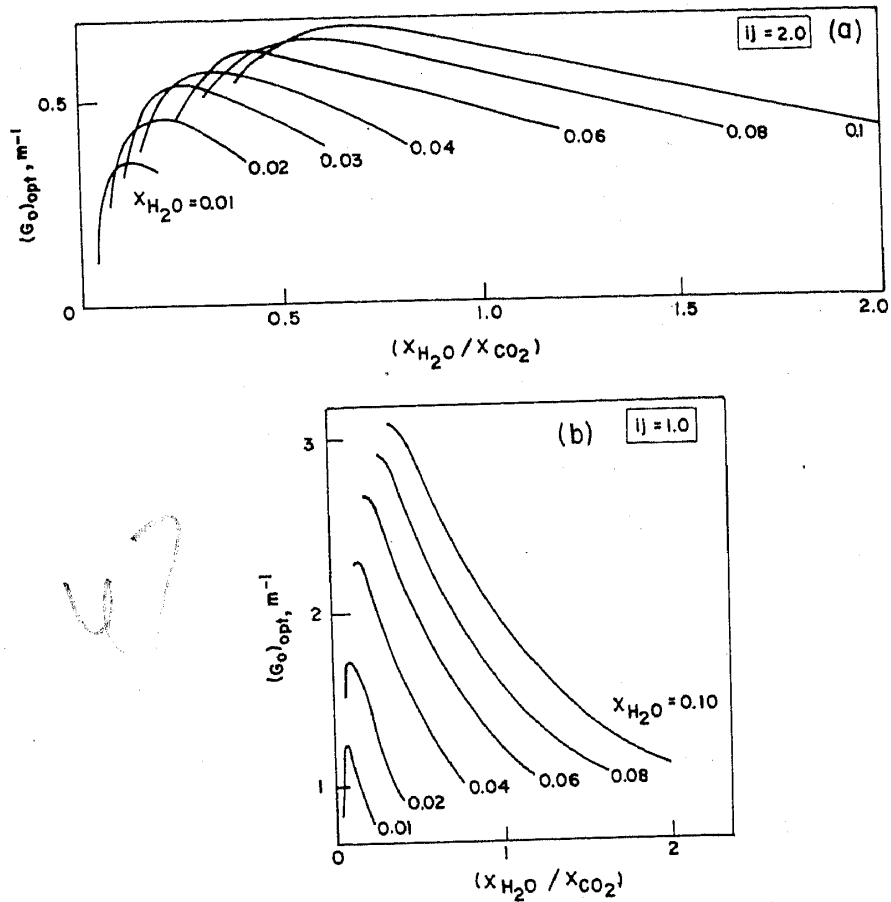
Figure 7. Effect of ratio of mole fractions of H_2O and CO_2 on optimum values of small-signal gain for **a.** $ij = 2$ and **b.** $ij = 1$.
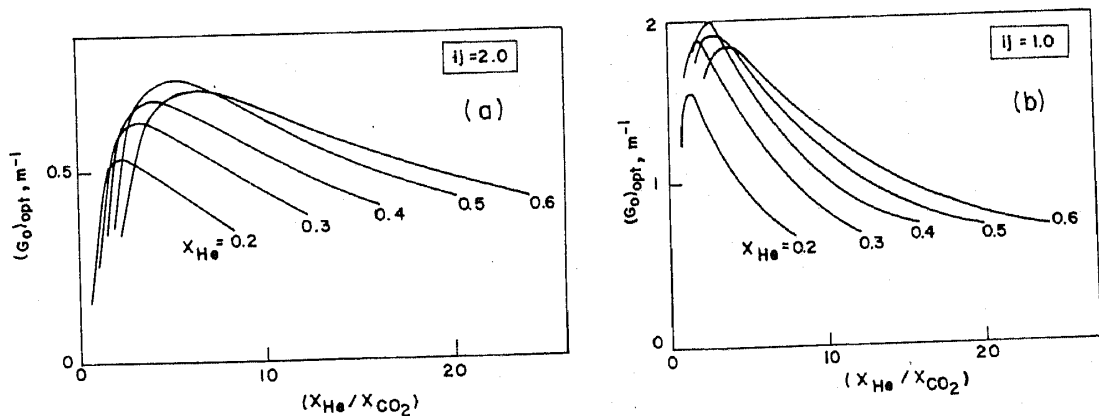

Figure 8. Effect of ratio of mole fractions of He and CO_2 on optimum values of small-signal gain for **a.** $ij = 2$ and **b.** $ij = 1$.

computed as a function of T'_0. The product $p'_0 L'$ is called the binary scaling parameter (Anderson 1976).

The appropriate optimum area ratio to be employed corresponding to the optimum value of $p'_0 L'$ to achieve the optimum gain on the $P(20)$ transition can be estimated in

the following way. First, for the given laser mixture and for the graphically known optimum value of χ_l, (1), (2), (18) and (19) are solved to obtain the optimum value of G_0 and also the value of ξ (to be designated as ξ_{opt}) at which it occurs. The value of $(G_0)_{opt}$ can also be read-off from the graphs presented in figures (7) and (8). Then it can be shown that (Reddy and Shanmugasundaram 1979a) the optimum area ratio A_{opt} and ξ_{opt} are related by the following expression:
for conical or hyperbolic nozzle,

$$[0 \cdot 5 - 0 \cdot 31(1 + \log_{10} A_{opt})^{-2}] A_{opt} = k_1^{-4} k_2 \exp(S_0 - \xi_{opt}) \tag{26}$$

and for wedge nozzle,

$$[1 \cdot 165 - 0 \cdot 56(0 \cdot 1 + \log_{10} A_{opt})^{-0 \cdot 2}] A_{opt} = k_1^{3 \cdot 37} k_2 \exp(S_0 - \xi_{opt}) \tag{27}$$

for the He catalyst and

$$[0 \cdot 669 - 0 \cdot 216(0 \cdot 194 + \log_{10} A_{opt})^{-0 \cdot 467}] A_{opt} = k_1^{3 \cdot 98} k_2 \exp(S_0 - \xi_{opt}) \tag{28}$$

for H_2O catalyst,
where k_1, k_2 and S_0 are functions of only T'_0. Hence for the known value of ξ_{opt}, either (26) or (27) or (28) can be solved for A_{opt} as a function of T'_0.

Thus, the optimum values can be obtained for the binary scaling parameter $p'_0 L'$ and the optimum area ratio A_{opt} for any given gas mixture composition and the nozzle shape. These values are computed for a wide range of gas compositions given in tables 1 and 2, however, we present the results only for few compositions in the form of graphs in figures 9 and 10. These graphs reveal that for any given gas composition, both $p'_0 L'$ and A increase monotonically with T'_0 for the following reason: since the specific energy of the gas mixture increases as T'_0 increases, it becomes necessary to expand the gas more so that the vibrational temperature (T_1) of the lower laser level (mode I), whose vibrational mode is coupled kinetically to the translational temperature, is reduced sufficiently. From figures 9 and 10 we notice a striking difference between systems 1
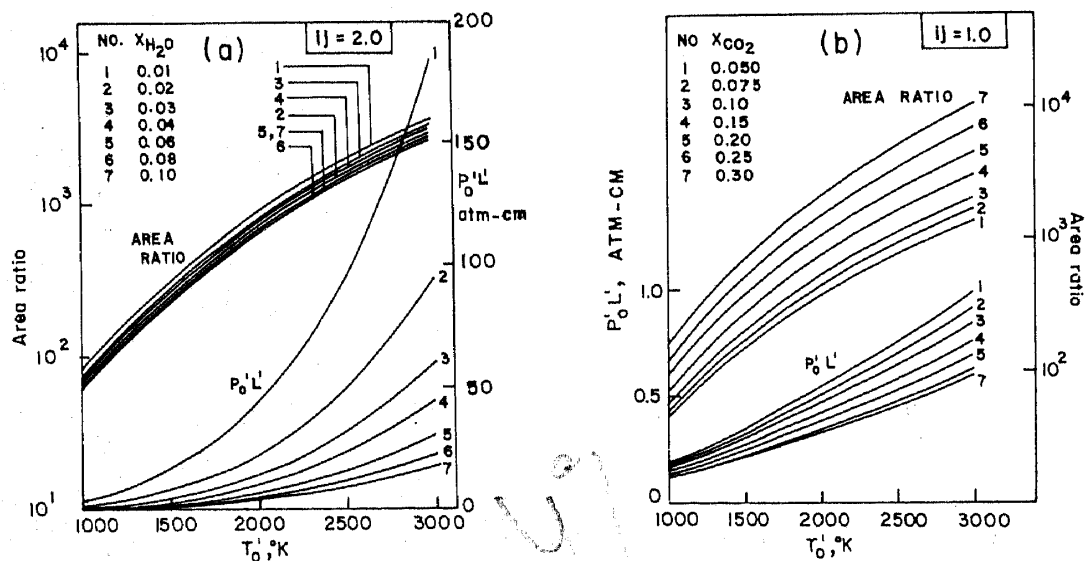

Figure 9. Variation of optimum area ratio and $p'_0 L'$, with reservoir temperature for **a.** $X_{CO_2} = 0 \cdot 15$; $ij = 2$ and **b.** $X_{H_2O} = 0 \cdot 1$; $ij = 1$ in system 1.
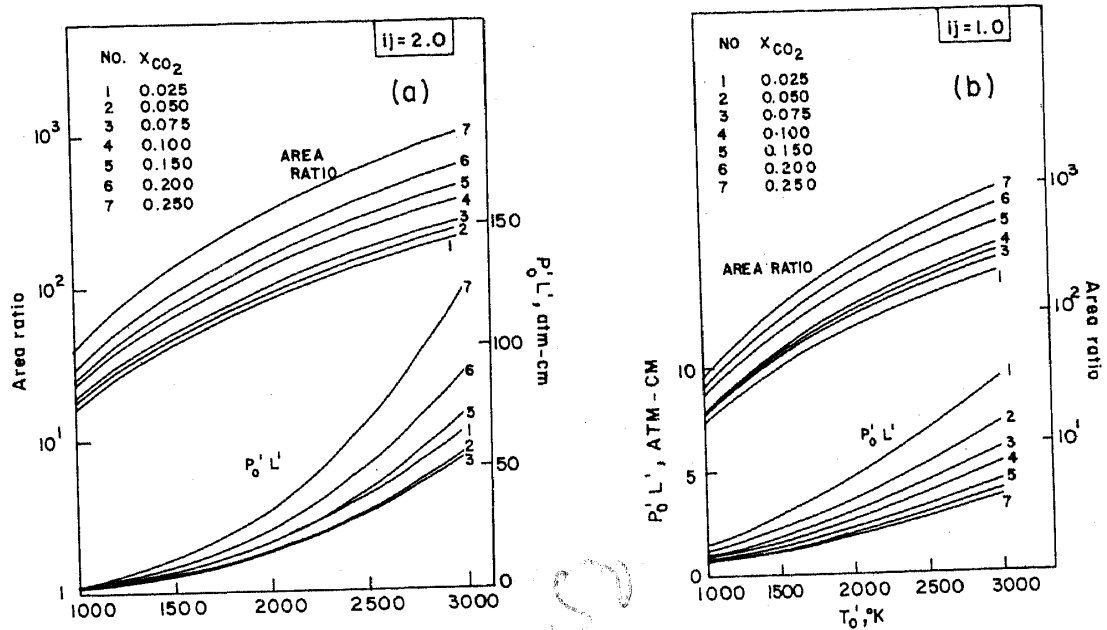
Figure 10. Variation of optimum area ratio and $p'_0 L'$, with reservoir temperature for **a.** $X_{He} = 0.5$; $ij = 2$ and **b.** $X_{He} = 0.4$; $ij = 1$ in system 2.

(H_2O catalyst) and 2 (He catalyst). The optimum values of A are in general much larger in system 1 than in system 2 and the optimum values of $p'_0 L'$ are of the same order in both the systems, for both wedge and conical or hyperbolic nozzles. This implies that system 1 is operationally superior to system 2 for the wedge nozzles, since the optimum value of G_0 is higher in system 1 than in system 2; whereas, system 2 is operationally superior to system 1 for conical or hyperbolic nozzle, since G_0 is lower in system 1 than in system 2.

Finally, it is important to note that for the very large values ($\sim 10^3$) of A_{opt} obtained in some of the cases, the pressure levels in the nozzle are likely to be very low ($\sim$ a few Torr) with the result that Doppler line broadening might dominate or become comparable to collisional (Lorentz) line broadening. Under such circumstances, the gas will be subjected to both Lorentz and Doppler line broadening mechanisms, either or neither of them dominating the scene, depending on the pressure level at any particular point in the flow field. Hence, a realistic approach would be to consider the full-line shape factor, incorporating both Lorentz and Doppler effects. This problem has been studied in detail and a relationship between the critical parameter reflecting the line-broadening mechanisms and some of the important parameters arising out of the gain optimization studies in CO_2-N_2 GDL is presented by Shanmugasundaram and Reddy (1980). Using this relationship it has been demonstrated that one would control the influence of the individual line-broadening mechanisms on the small-signal gain output by judiciously choosing the value of this critical parameter.

Further, at very low gas densities rapid intra-mode coupling of vibrational states, fundamental to the two-mode model of Anderson which has been adopted in the present analysis, might be lost. Under such a situation a much more detailed analysis of the molecular kinetics would need to be invoked. Also, if very low translational temperatures are obtained because of large expansion ratios, then additional concerns

arise. These are (a) the fact that inadequate vibrational relaxation kinetic data exist to support the extrapolation of the simplified (τp) correlations to very low gas temperatures, and (b) that maximum small-signal gain would be expected to shift far away from $P(20)$ to much lower P-branch, transitions, as dictated by the Boltzmann distribution of the rotational-state populations.

4. Conclusion

The dependence of the performance of a GDL which is characterised by a small-signal optical gain, on a large number of system parameters has been discussed. A survey of the efforts to obtain optimal conditions by varying a certain parameter separately, other parameters remaining constant by various authors is presented. We have pointed out that the optimization of the GDL performance this way is very tedious and time consuming and the only alternative is to optimize all the parameters simultaneously. A comprehensive theoretical analysis of gain-optimization of $10 \cdot 6$ μm CO_2-N_2-H_2O or He GDL using wedge or conical or hyperbolic nozzle shapes is presented in this paper. In the analysis presented here, the equations governing the steady inviscid non-reacting GDL flow in a supersonic nozzle are considered in their universal form in which the solutions depend on a single parameter which combines all the other parameters of the problem. Similar solutions are obtained for both CO_2-N_2-H_2O and CO_2-N_2-He gasdynamic laser systems with different nozzle shapes and are used to optimize the small-signal gain coefficient G_0 on a $P(20)$ $(001) \rightarrow (100)$ transition at $10 \cdot 6$ μm wavelength and the universal correlating parameter χ_I and the results are presented in the form of graphs. These results are further used to compute the optimum values for the area ratio A and the binary scaling parameter, $p'_0 L'$, as functions of reservoir temperature which are also presented in the form of graphs for various gas mixture compositions. Since L' is a function of the nozzle throat height and the expansion angle, the said $p'_0 L'$ values can be used to estimate the optimum reservoir pressures for a wide range of nozzle sizes.

From the above analysis we have shown that small signal optical gains as high as $3 \cdot 1$ m^{-1} can be achieved on the $P(20)$ line of the $(001) \rightarrow (100)$ transition by employing wedge nozzles in CO_2-N_2-H_2O systems for the gas mixture $CO_2:N_2:H_2O$ $= 30:60:10$ (%). Similarly, in CO_2-N_2-He system an optimum value of 2 m^{-1} gain can be obtained for a composition of $CO_2:N_2:He = 15:45:40$ (%). The gain values are relatively smaller for both the systems when conical or hyperbolic nozzles are employed; for example, the optimum value of gain that can be obtained is $0 \cdot 7$ m^{-1} in CO_2-N_2-H_2O system by using the gas mixture $CO_2:N_2:H_2O = 15:75:10$ (%) and the corresponding value in CO_2-N_2-He system is $0 \cdot 75$ m^{-1} for the gas composition $CO_2:N_2:He = 10:40:50$ (%). The analysis further predicts that CO_2-N_2-H_2O GDL system is operationally superior to CO_2-N_2-He system when wedge nozzles are used while the converse is true for conical or hyperbolic nozzle shapes.

References

Anderson Jr J D 1970 *Phys. Fluids* **14** 1983
Anderson Jr J D 1975 *Acta Astronautica* **2** 911
Anderson Jr J D 1976 *Gasdynamic lasers. An introduction* (New York: Academic Press)

Basov N G and Oraevskii A N 1963 *Sov. Phys.-JETP* **17** 1171
Christiansen W H, Russel D A and Hertzberg A 1975 *Annu. Rev. Fluid Mech.* **7** 115
Gerry E T 1970 *IEEE Spectrum* **7** 51
Hurle I R and Hertzberg A 1965 *Phys. Fluids* **8** 1601
Kantrowitz A R 1946 *J. Chem. Phys.* **14** 150
Konyukhov V K and Prokhorov A M 1966 *JETP Lett.* **3** 286
Losev S A and Makarov V N 1975 *Sov. J. Quantum Electron.* **4** 905
Losev S A 1981 *Gasdynamic laser* (New York: Springer-Verlag)
Mcmanus J I and Anderson Jr J D 1976 *AIAA J.* **14** 1770
Reddy K P J and Reddy N M 1984 *J. Appl. Phys.* **55** 51
Reddy N M and Shanmugasundaram V 1979a *J. Appl. Phys.* **50** 2565
Reddy N M and Shanmugasundaram V 1979b *J. Appl. Phys.* **50** 2576
Reddy N M and Shanmugasundaram V 1979c *Proc. Second Int. Symp. on gasflow and Chemical Lasers* (ed.)
    J F Wendt (Washington: Hemisphere Publ. Corp.) 319
Shanmugasundaram V and Reddy N M 1980 *J. Appl. Phys.* **51** 5615
Shanmugasundaram V and Reddy N M 1983 *Pramana* **21** 131